

Dating stratigraphic variations of ions and oxygen isotopes in a high-altitude snowpack by comparison with daily variations of precipitation chemistry at a low-altitude site

W.H. Theakstone

ABSTRACT

Daily precipitation at Tustervatn (65°83'N, 13°92'E, 439 m above sea level) was analysed for ions and oxygen isotopes. Seven-day air mass trajectories provided information about the precipitation source and history. The highest Na⁺ loads were associated with air masses which had crossed the Norwegian Sea and the highest non-sea-salt SO₄²⁻ loads with trajectories crossing Scandinavia or the United Kingdom; high SO₄²⁻ loads in late April reflected decreasing snow cover. Trajectories from the Arctic basin resulted in the lowest δ¹⁸O values. During the winter, 4.8 m of snow accumulated at 1470 m above sea level on the glacier Austre Okstindbreen, 25 km north-east of Tustervatn. Mean ionic concentrations were lower than at Tustervatn, but loads were higher, as the total precipitation was three times greater. At both sites, ionic loads were closely related to ionic concentrations but not to sample water-equivalent values/precipitation amounts. Dates could be assigned to much of the snowpack on the basis of similarities between its chemical stratigraphy and temporal variations of precipitation chemistry at Tustervatn. Examination of the influence of individual storms on δ¹⁸O variations and the relationship between those variations and atmospheric circulation patterns has potential importance in relation to understanding past, present and possible future climatic conditions.

Key words | air mass trajectories, ionic concentrations, Norway, oxygen isotopes, precipitation chemistry, snowpack stratigraphy

W.H. Theakstone

School of Environment and Development,
University of Manchester,
Manchester M13 9PL,
UK

Tel.: +44 161 275 3674, 3641;

Fax: +44 161 275 7878

E-mail: wilfred.theakstone@manchester.ac.uk

INTRODUCTION

The coupling between atmospheric circulation and precipitation/snow accumulation is of interest in relation to both current and possible future climatic conditions (Araguas-Araguas *et al.* 2000). Regional-scale processes, such as the trajectories of the transport of water vapour and the rainout history of the air masses responsible for the precipitation, have a primary control on the isotopic composition of local precipitation (Rozanski *et al.* 1982). Because the oxygen isotopic composition of precipitation is a tracer of atmospheric moisture transport systems (Hoffmann *et al.* 2000; Yoshimura *et al.* 2004), studies of the stable isotopic composition of precipitation have greatly

aided in the understanding of the source and transport of moisture in the atmosphere (Dansgaard 1964; Gat 1996; Fricke & O'Neil 1999).

Seasonal variations of precipitation δ¹⁸O values have been used to document changes of climate over time (Cuffey *et al.* 1995) and to date ice cores (Hammer *et al.* 1978). However, because changes of vapour source regions and air mass mixing influence the temporal variations of precipitation δ¹⁸O values (Cole *et al.* 1999; Aizen *et al.* 2005), interpretation of the ice core record requires an understanding of the manner in which the δ¹⁸O values at a site are related to atmospheric circulation and air mass

doi: 10.2166/nh.2008.039

trajectories (Kahl *et al.* 1997). Aggregate data, such as the monthly averages in the dataset of the International Atomic and Energy Agency (IAEA) Global Network of Isotopes in Precipitation (GNIP), do not permit examination of the influence of individual storms on the $\delta^{18}\text{O}$ record (Rozanski *et al.* 1993; Burnett *et al.* 2004). For this, observations of within-a-season variations of precipitation $\delta^{18}\text{O}$ values, and of their relationship to atmospheric circulation patterns, are needed.

Long-range transport of air pollutants results in ionic variations within accumulating snow (Maupetit & Delmas 1994) and analyses of the ionic composition of precipitation can provide information about both contaminant sources and the processes of their transport and deposition (Raben *et al.* 2000; Norman *et al.* 2001; Krupa 2002; Asaf *et al.* 2005). Combining investigations of the ionic and isotopic compositions of precipitation at a site in relation to synoptic conditions can provide evidence about multiple sources of moisture and their associated transport routes (Aizen *et al.* 2005).

In an attempt to throw light on these matters, studies were undertaken at two sites close to the Arctic Circle in Norway (Figure 1). Throughout the 1997–98 winter, oxygen isotopes and ions in precipitation at Tustervatn (65° 83'N, 13° 92'E, 439 m above sea level) were sampled on a daily basis. The trajectories of the air masses responsible for precipitation were examined. Towards the end of the winter, on 6 May, samples were collected from the snowpack which had accumulated at 1470 m above sea level on the glacier Austre Okstindbreen, 25 km north-east of Tustervatn; Austre Okstindbreen (12 km²) is the largest of the 15 glaciers of Okstindan, an area of alpine-type topography some 60 km south of the Arctic Circle and about 80 km from the Norwegian Sea (Figure 1). Stratigraphic variations of oxygen isotopes and ions in the snowpack were compared with temporal variations in the precipitation at Tustervatn, in an attempt to establish the chronology of snow accumulation at the higher site. The good temporal resolution of the event-based ('daily') data from Tustervatn, together with the results of air mass trajectory analyses, permitted evaluation of the relationship of $\delta^{18}\text{O}$ values to synoptic weather systems and provided a basis for dating elements of the stratigraphy of the snowpack at 1470 m.

DATA COLLECTION AND BACKGROUND INFORMATION

Tustervatn

Precipitation samples have been collected at Tustervatn on a daily basis, at 07:00 hours local time, since 1973, as part of the Norwegian Monitoring Programme for Long-Range Transported Air Pollutants (Tørseth & Semb 1995). The nature of the precipitation (snow/rain) is recorded. Tustervatn is in a rural area, uninfluenced by local anthropogenic emission sources. The site, and the methods used in monitoring dry and wet deposition were described by Tørseth & Semb (1995) and Tørseth *et al.* (1999). In dry periods, the precipitation sampler (diameter: 0.2 m) is left open, but is washed daily with distilled water in order to avoid contamination by dry deposition. If more than about 1 mm of precipitation is collected, ionic concentrations (Cl^- , SO_4^{2-} , NO_3^- , Na^+ , Mg^{2+} , Ca^{2+} , K^+ , NH_4^+ , H^+ [pH]) are measured by the Norwegian Institute for Air Research (NILU). The total chemical load for each day is calculated as the product of the mean concentration and total precipitation. Throughout the 1997–98 winter, circumstances permitting, a second sample of precipitation was collected whenever the daily precipitation exceeded 2 mm; oxygen isotope analysis of these samples was undertaken at the Niels Bohr Institute, University of Copenhagen. 92% of the total precipitation was analysed for oxygen isotopes.

Tørseth *et al.* (1999) reported that, for the period 1993–96, the very good correspondence between Na^+ and Mg^{2+} in precipitation at Tustervatn ($R^2 = 0.97$) indicated that there were no significant sources for these compounds other than sea-spray. The very high correlations between Na^+ , Cl^- and Mg^{2+} concentrations in 1997–98 winter precipitation (Table 1) again indicated their source as sea-spray. The relatively high inputs of sea-salt ions at Tustervatn are supplied principally by wet deposition (Raben *et al.* 2000). Wet scavenging is also the most important process leading to the deposition of non-sea-salt sulfate (nssSO_4^{2-}), calculated as $\text{nssSO}_4^{2-} = \text{SO}_4^{2-} - 0.252 \text{Na}^+$ (Raben *et al.* 2000). nssSO_4^{2-} concentrations in the Okstindan region are amongst the lowest in Europe (Tørseth *et al.* 1999), having fallen by 62% from 1980 to

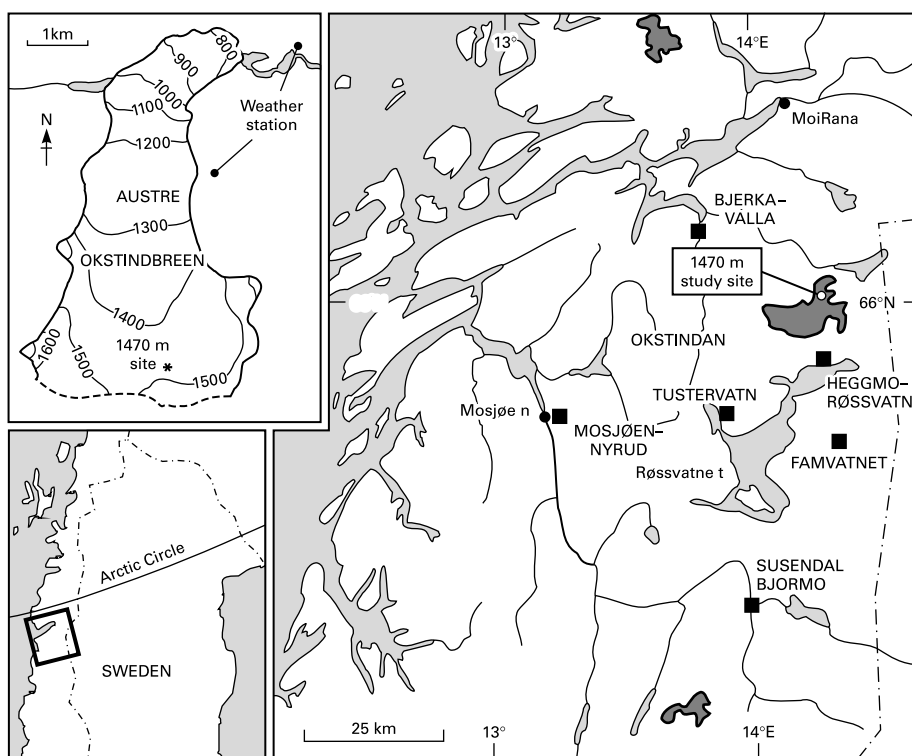


Figure 1 | The Okstindan area, Norway. Dark shading indicates glacier-covered areas. Light shading indicates lakes and the ocean. Towns are shown by circles and DNMI precipitation stations by squares. Air temperatures are recorded at Susendal Bjormo. Samples for chemical analysis were collected at Tustervatn and the 1470 m site. The insets show the glacier Austre Okstindbreen and the location of the Okstindan area.

1995 as a result of reduced SO_4^{2-} emissions in Europe (Tørseth 1996). Raben *et al.* (2000) reported that, during the 1994–95 winter, the air masses which brought high nssSO_4^{2-} loads to Tustervatn arrived from the south, having had a lengthy passage over land; they concluded that the SO_4^{2-} ions supplied by those events had a continental origin.

Austre Okstindbreen

From 1980 until 1995, Austre Okstindbreen was the principal focus of the Okstindan Glacier Project, a collaborative programme of the Universities of Manchester, UK and Aarhus, Denmark. Annual mass balance observations (Knudsen 2000) and investigations of the chemistry of the river water issuing from the glacier (Theakstone 1988;

Table 1 | Correlation (R^2 values) between ionic concentrations in precipitation at Tustervatn, October 1997–May 1998

	Na	Cl	Mg	Ca	SO ₄	K	NO ₃	NH ₄	nssSO ₄
Na		1.00	0.99	0.61	0.46	0.31	0.02	0.01	0.00
Cl			0.99	0.60	0.45	0.32	0.01	0.02	0.00
Mg				0.62	0.46	0.25	0.01	0.01	0.00
Ca					0.67	0.31	0.05	0.20	0.12
SO ₄						0.21	0.29	0.23	0.49
K							0.01	0.35	0.01
NO ₃								0.26	0.37
NH ₄									0.56
nssSO ₄									

Theakstone 2003; Theakstone & Knudsen 1996a, b) demonstrated the importance of year-to-year variations of the winter-accumulated snowpack. Studies of the chemical stratigraphy of the snowpack showed the strong influence of both atmospheric circulation patterns and air temperature during precipitation (He & Theakstone 1994). Concentrations of Mg^{2+} , K^+ and Ca^{2+} in the pre-melt snowpack were closely related to those of Na^+ (Raben & Theakstone 1998). Stratigraphic differences of ions and oxygen isotopes were marked (Raben & Theakstone 1994) but, in general, the strata could neither be assigned precise dates nor linked to particular events or precipitation source areas. However, evidence of the strong influence of differing synoptic patterns was provided by analysis of the ionic variations in the 7 m of snow which accumulated at 1470 m asl during the 1994–95 winter (Raben *et al.* 2000). The thickness of the snowpack at the 1470 m site was determined towards the end of each winter from 1986 until 1995, as part of the mass balance programme at Austre Okstindbreen; water-equivalent (WE) values ranged from 1.8 m to 4.0 m.

On 6 May 1998, a 5.2 m deep pit was excavated from the surface of the Austre Okstindbreen snowpack at 1470 m asl. The surface gradient at the site was less than 2%. The 1997 summer surface was observed at a depth of 4.8 m. A core, 1.5 m long, was taken from the bottom of the pit. 134 samples, each 0.05 m long, were collected from the pit walls and core for subsequent laboratory analysis. In order to avoid contamination, protective clothing was worn during sampling. Samples were allowed to melt in sealed polythene bags before being transferred to pre-cleaned polyethylene flasks and vials. Before transport to the laboratories, they were kept in snow at 0°C in black plastic bags to prevent penetration of daylight. In the laboratories, they were stored in a dark room at 2–4°C. Because of the low particulate content in the snow, filtration was not carried out. Samples were sent to the University of Copenhagen Niels Bohr Institute for oxygen isotope analyses and to the Aarhus University Earth Sciences Institute for ionic (Na^+ and SO_4^{2-}) analyses.

The onset of the 1997–98 winter

Daily temperature data are collected for the Norwegian Meteorological Institute (DNMI) at Susendal-Bjormo

(265 m asl), some 35 km south of Tustervatn (Figure 1). Between 1987 and 1989, and from 1990 until 1993, automatic weather stations were operated at Austre Okstindbreen. Mean daily temperatures at the stations correlated well with those at Susendal-Bjormo (November 1987–May 1989: $n = 559$, $R^2 = 0.75$; October 1990–July 1993: $n = 1012$, $R^2 = 0.87$). Temporal variations of air temperature at the glacier during the 1997–98 winter are assumed to have been similar to those at the DNMI station. Data from Susendal-Bjormo, used together with a lapse rate of 0.6°C per 100 m, indicate that the temperature at 1470 m remained consistently below 0°C from early October until early May. The temperature decreased markedly from 7 October to 11 October, and October 8 is regarded as the most likely date on which net accumulation of snow began at 1470 m on Austre Okstindbreen.

RESULTS AND DATA ANALYSIS

Tustervatn

Precipitation fell at Tustervatn on 108 days between 8 October 1997 and 6 May 1998. The total precipitation was 0.816 m. Precipitation data are collected for the DNMI at several stations within 35 km of Tustervatn (Figure 1). From 8 October 1997 to 6 May 1998, the totals at Famvatnet (510 m asl), Heggmo-Røssvatn (399 m asl), Susendal-Bjormo (265 m asl), Bjerka-Valla (20 m asl) and Mosjøen-Nyrud (5 m asl) were 0.509 m, 0.940 m, 0.733 m, 0.806 m and 1.218 m, respectively, and daily values at each of these sites were well correlated with those at Tustervatn ($R^2 = 0.84, 0.84, 0.82, 0.76$ and 0.71 , respectively). The temporal patterns at the six stations were very similar, with a high proportion of the overall winter precipitation falling in January and February. The pattern of winter precipitation at 1470 m asl on Austre Okstindbreen is assumed to have been similar to that at the DNMI stations and, given the consistently low temperatures throughout the period, it is highly likely that all the precipitation there was as snow.

Samples for ionic analysis were collected at Tustervatn on 94 days between 8 October 1997 and 6 May 1998, during which the precipitation (0.792 m) was 97.1% of the overall total. Ionic loads were assigned to the date on which precipitation collection started at 07:00 hours, and

the contribution of each sample to the total (8 October–6 May) load was calculated. Na^+ concentrations ranged from 0.06 mg L^{-1} to 23.42 mg L^{-1} ; daily Na^+ loads were even more variable, as reflected in a larger coefficient of variation (Table 2). The total Na^+ load was $1797.46 \text{ mg m}^{-2}$. nssSO_4^{2-} concentrations ranged from 0.00 mg L^{-1} to 2.01 mg L^{-1} and the total nssSO_4^{2-} load was 65.95 mg m^{-2} (Table 2).

The first notable Na^+ loads were those of 19 and 20 October (Figure 2). Na^+ loads were low throughout November, December and January, but were higher for most of February; the winter's highest value (269 mg m^{-2}) was that of 10 February (Figure 2). The last period of high Na^+ loading was in mid-March, with a maximum of 247 mg m^{-2} on 19 March. Relatively high proportions of the winter's total nssSO_4^{2-} load arrived on 25–26 January, 21 February and 25 February (Figure 3). Late April produced further high loads despite rather low precipitation.

Samples for isotopic analysis were collected at Tustervatn on 73 of the 108 days between 8 October 1997 and 6 May 1998; the precipitation of those days (0.751 m) was 92.0% of the total for the period. Most of the winter months were characterised by marked variations of pre-

cipitation $\delta^{18}\text{O}$ values (Figure 4). The average daily value was -13.11‰ (Table 1); the minimum (-28.62‰) was that of 4 March, the maximum (-4.66‰) that of 17 December. The relationship between the 73 values and the mean daily temperature (T) at Susendal-Bjormo was $\delta = (0.48T - 12.60)\text{‰}$. Although the relationship between temperature and $\delta^{18}\text{O}$ values was as expected – the lower the temperature, the more ^{18}O -depleted the precipitation – the correlation was low ($R^2 = 0.18$). Given the influence of factors other than temperature on precipitation $\delta^{18}\text{O}$ values (Fricke & O'Neil 1999) and the 35 km separation of the two sites, this was unsurprising.

Austre Okstindbreen

Densities of every 0.15 m increment of snow and firn were determined in order to calculate the water-equivalent (WE) thickness of the samples. Temperature was measured at 0.05 m intervals between the surface and the base of the 5.2 m pit. Density generally increased with depth, to around 530 kg m^{-3} at the 1997 summer surface and 640 kg m^{-3} in the lowermost sampled firn (Figure 6). The WE thickness of

Table 2 | Ionic concentrations, ionic loads and oxygen isotopic values of daily precipitation at Tustervatn (top) and the snowpack at 1470 m asl on Austre Okstindbreen (bottom). The coefficient of variation (standard deviation/mean) indicates the homogeneity of the sample values

Tustervatn	Precipitation (mm)	Na^+ concn. (mg L^{-1})	Na^+ load (mg m^{-2})	nssSO_4^{2-} concn. (mg L^{-1})	nssSO_4^{2-} load (mg m^{-2})	$\delta^{18}\text{O}$ (‰)
Total	791.69		1797.46		65.95	
Mean	8.42	1.78	18.92	0.14	0.71	-13.11
Standard deviation	8.33	3.08	43.18	0.26	0.91	4.97
Coeff. of variation	0.99	1.73	2.28	1.86	1.28	-0.38
Maximum	54.49	23.42	269.33	2.01	4.86	-4.66
Minimum	0.80	0.06	0.17	0.00	0.04	-28.62
<i>n</i>	94	94	94	94	94	73
1470 m	Water equivalent (mm)	Na^+ concn. (mg L^{-1})	Na^+ load (mg m^{-2})	nssSO_4^{2-} concn. (mg L^{-1})	nssSO_4^{2-} load (mg m^{-2})	$\delta^{18}\text{O}$ (‰)
Total	2301.89		2000.61		379.40	
Mean	23.98	0.86	20.84	0.17	3.95	-12.85
Standard deviation	3.46	1.03	25.23	0.30	6.83	2.80
Coeff. of variation	0.14	1.20	1.21	1.79	1.73	-0.22
Maximum	32.08	6.21	151.80	2.01	45.28	-7.86
Minimum	6.89	0.04	0.47	0.00	0.00	-24.04
<i>n</i>	96	96	96	96	96	96

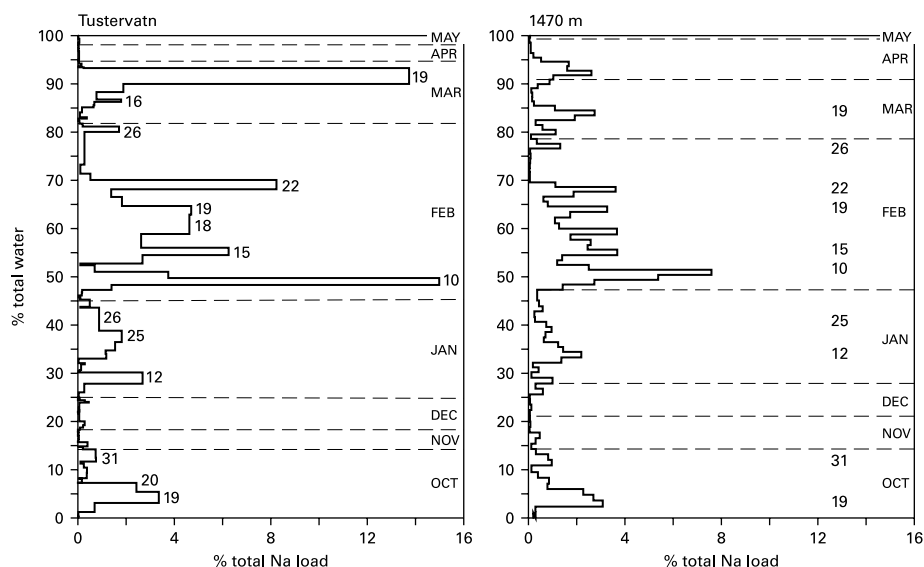


Figure 2 | Left: daily precipitation and Na^+ loads at Tustervatn as percentages of the 8 October 1997–6 May 1998 total. Dates of some events are indicated. Right: water-equivalent heights of snowpack samples above the 1997 summer surface at 1470 m asl on Austre Okstindbreen and Na^+ loads in the samples as percentages of the total. Suggested dates of accumulation of some snowpack samples are shown.

the 1997–98 snowpack, determined from the density data, was 2.30 m. The temperature of the uppermost 0.14 m of snow at the 1470 m site was close to the melting point. That of the underlying snow declined to a minimum of 5.8°C at 2.7 m below the surface and then increased to 3.5°C at 5.2 m (Figure 5). The low temperatures, the absence of ice layers and the lack of abrupt density variations (Figure 5)

indicated that there had been very limited surface melting and/or refreezing of percolating meltwater within the snowpack during the winter.

The Na^+ load of each of the 96 snowpack samples was calculated as the product of the measured concentration and the WE value of the sample. Concentrations ranged from 0.04 mg L⁻¹ to 6.21 mg L⁻¹ (Table 2); the mean load

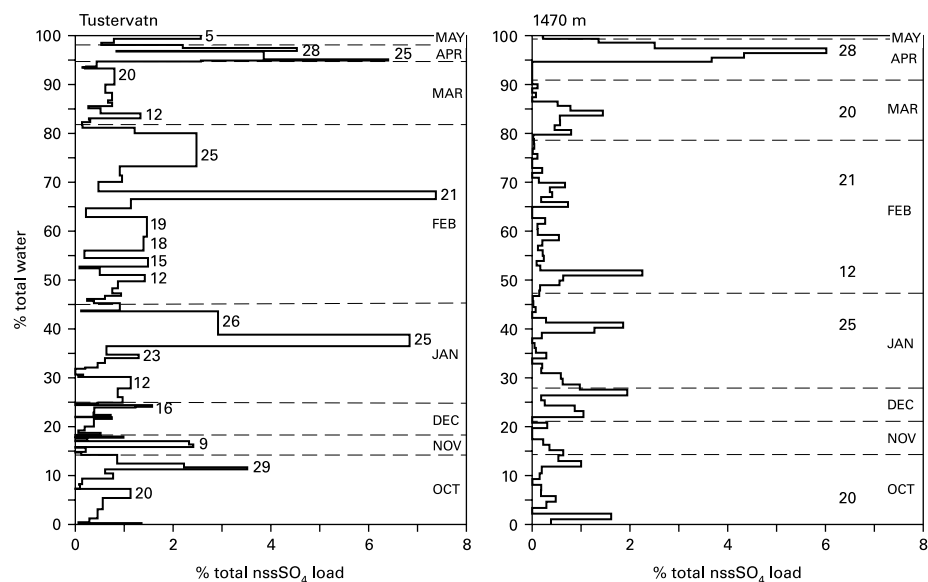


Figure 3 | Left: daily precipitation and nssSO_4^{2-} loads at Tustervatn as percentages of the total between 8 October 1997 and 6 May 1998. Dates of arrival of particular loads at Tustervatn are indicated. Right: water-equivalent heights of snowpack samples above the 1997 summer surface at 1470 m asl on Austre Okstindbreen and nssSO_4^{2-} loads in the samples as percentages of the total. Suggested dates of accumulation of some snowpack samples are shown.

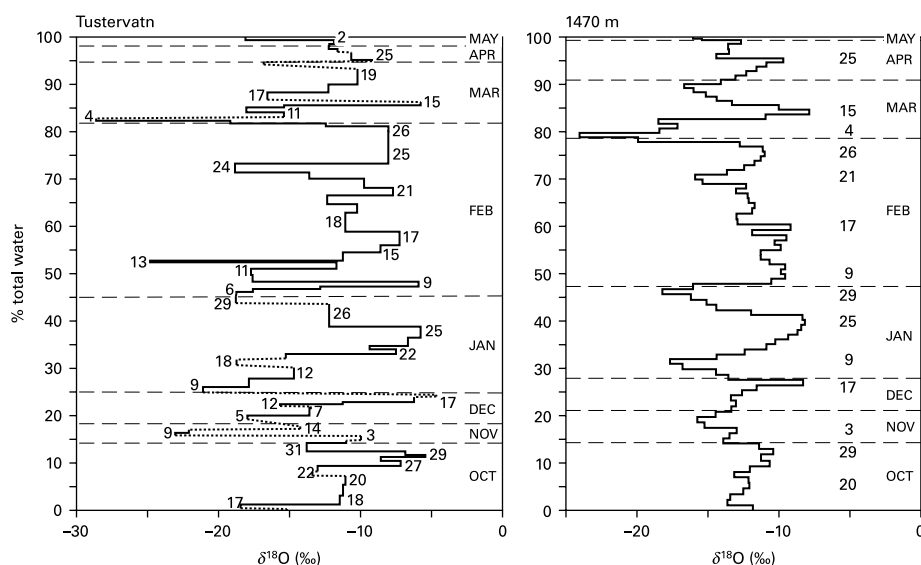


Figure 4 | Left: $\delta^{18}\text{O}$ values of precipitation collected at 07:00 hours at Tustervatn plotted against the incremental precipitation between 8 October 1997 and 6 May 1998. Dates of collection are shown. Gaps in the record (dotted lines) represent days with < 2 mm of precipitation. Left: $\delta^{18}\text{O}$ values of snowpack samples at 1470 m asl on Austre Okstindbreen plotted against the incremental water-equivalent height above the 1997 summer surface. Suggested dates of accumulation of some snowpack samples are shown.

was 20.84 mg m^{-2} . The mean nssSO_4^{2-} load was 3.95 mg m^{-2} (Table 2), but only 77 of the samples had a measurable load: their mean nssSO_4^{2-} load was 4.93 mg m^{-2} . The percent contribution of each sample to the overall Na^+ and nssSO_4^{2-} loads was determined. The results, plotted against the percent WE height above the 1997 summer surface (WEOD), are shown in Figures 2 and 3. Na^+ loads were highest between about 50% and 70% WEOD (Figure 2), whilst the highest nssSO_4^{2-} loads were close to the top of the snowpack (Figure 3).

The oxygen isotope analyses confirmed the on-site identification of the location of the 1997 summer surface: the reduced amplitude of the $\delta^{18}\text{O}$ variations below it (Figure 5) reflected the homogenisation that accompanies the snow–firn–ice transformation. The mean $\delta^{18}\text{O}$ value of the 96 samples from the winter snowpack was -12.85‰ (Table 2). The minimum (-24.04‰) was at a below-surface depth of 1.15–1.20 m (Figure 5), equivalent to around 79% WEOD (Figure 4). The maximum value (-7.86‰) was at 0.90–0.95 m depth, around 84% WEOD (Figure 4).

Air mass trajectories to Tustervatn

Many studies of air and precipitation chemistry have made use of trajectories to determine pollutant source regions and

transport pathways (Dorling *et al.* 1992; Kahl *et al.* 1997). Seven-day trajectories of air masses arriving at Tustervatn, computed with the FLEXTRA trajectory model (Stohl *et al.* 1995), provide information about the source and history of the precipitation. Trajectories arriving at 500 m asl at Tustervatn at 18:00 hours, approximately midway through the daily period of precipitation sampling, were chosen for analysis.

Trajectories associated with the highest Na^+ loads approached Tustervatn from the west, having passed across the Norwegian Sea (Figure 6(a)); all had their ‘origin’ north of 65°N and most arrived at Tustervatn in February or March. Most of the highest nssSO_4^{2-} loads were associated with trajectories which had crossed the land masses of Scandinavia or the United Kingdom (Figure 6(b)); three of the seven arrived at Tustervatn in April. Twelve of the daily precipitation samples at Tustervatn had $\delta^{18}\text{O}$ values of -8.0‰ or more; the associated 7-day trajectories varied widely, with ‘origins’ as far south as 40°N , but most arrived at Tustervatn from the west or south-west (Figure 6(c)). $\delta^{18}\text{O}$ values of -18.0‰ or less were recorded for 12 of the samples; most of the associated 7-day trajectories ‘originated’ over the Arctic basin, crossing the Greenland or Barents Seas on the way to Tustervatn (Figure 6(d)). There was no clearly discernible temporal pattern in the occurrence of the highest and lowest $\delta^{18}\text{O}$ values.

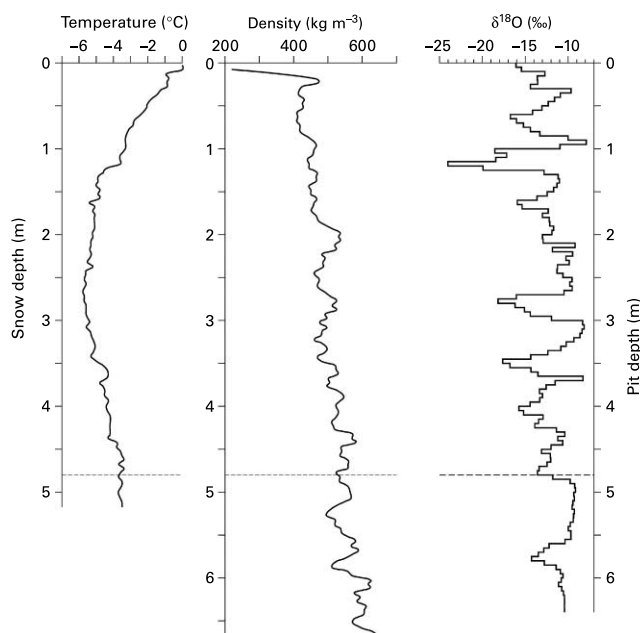


Figure 5 | Temperature, density and isotopic composition of the snowpack and underlying firm at Austre Okstindbreen, 6 May 1998. The sampling site was 1470 m above sea level. The 1997 summer surface, indicated by a broken line, was visible at a depth of 4.8 m.

DISCUSSION

Ionic concentrations and ionic loads at Tustervatn and Austre Okstindbreen

Daily chemical loading at Tustervatn is more dependent on ionic concentrations than on the amount of precipitation. Accordingly, the relationship between Na^+ concentrations and Na^+ loads in the 94 samples ($R^2 = 0.78$) was much stronger than that between precipitation amounts and the Na^+ loads ($R^2 = 0.17$), and the relationship between nssSO_4^{2-} concentrations and nssSO_4^{2-} loads ($R^2 = 0.41$) was stronger than between precipitation amounts and the nssSO_4^{2-} loads ($R^2 = 0.09$).

The concentration of sea-salt particles decreases markedly with altitude above the sea surface, and a very high frequency of precipitation helps to maintain low concentrations of particles in air. Nickus *et al.* (1997) noted that, because of the general increase of precipitation with height, loads deposited on glaciers in the European Alps and those deposited in the lower valleys were of the same order of magnitude, despite the lower pollutant concentrations at high alpine sites. Similarly, although the mean Na^+ concen-

tration at 1470 m was less than half that at Tustervatn, the total Na^+ load was some 11% higher, as precipitation was almost three times that at the lower site (Table 1). The same was the case during the 1994–5 winter (Raben *et al.* 2000).

The relationship between the Na^+ concentrations and Na^+ loads of the 96 samples from the 1470 m site was very strong ($R^2 = 0.99$), whilst that between the WE values of the samples and their Na^+ loads was weak ($R^2 = 0.02$). As 60% of the total nssSO_4^{2-} load was supplied by only 13 of the 96 samples, the absence of a significant relationship between the WE values of the samples and both the nssSO_4^{2-} concentrations and the nssSO_4^{2-} loads is not surprising.

Maupetit & Delmas (1994) noted that a sharp increase in the impurity content of snow in higher areas of the European Alps occurred in spring as a result of the upward transport of ions from lower-altitude polluted regions. The winter snow cover also reduces some natural sources. Towards the end of the winter season, the declining snow cover and the growing vegetation result in new sources from which trace substances, including nssSO_4^{2-} , are lifted up by convection and up-slope winds into the growing mixed layer of the lower atmosphere (Preunkert *et al.* 2000). By late April, the snow cover having melted from much of southern Scandinavia, the air masses arriving at Okstindan (Figure 6(b)) would have traversed areas offering greater opportunities for the acquisition of nssSO_4^{2-} . Although the mean nssSO_4^{2-} concentration at 1470 m was only 20% higher than that at Tustervatn, the total nssSO_4^{2-} load was very much larger (Table 1). This reflected the contribution of late-winter values (Figure 3). Transport of aerosol particles in the planetary boundary layer from mid-latitude industrial areas to the Arctic in winter and spring results in the formation of arctic haze. This peaks in the spring, and the components of the haze may be retained for several weeks if not removed by snow, rain or turbulent air. Although arctic haze is a possible source of nssSO_4^{2-} deposition at Tustervatn, long-term studies (Tørseth *et al.* 1999) and the trajectory analyses reported here, suggest that its contribution is not significant.

Chemical load, or flux, calculations pertaining to ice cores often are precluded by uncertainties, such as density variations and the timing of chemical inputs. The results of this study, showing that ionic loads are much more strongly related to the ionic composition of precipitation than to

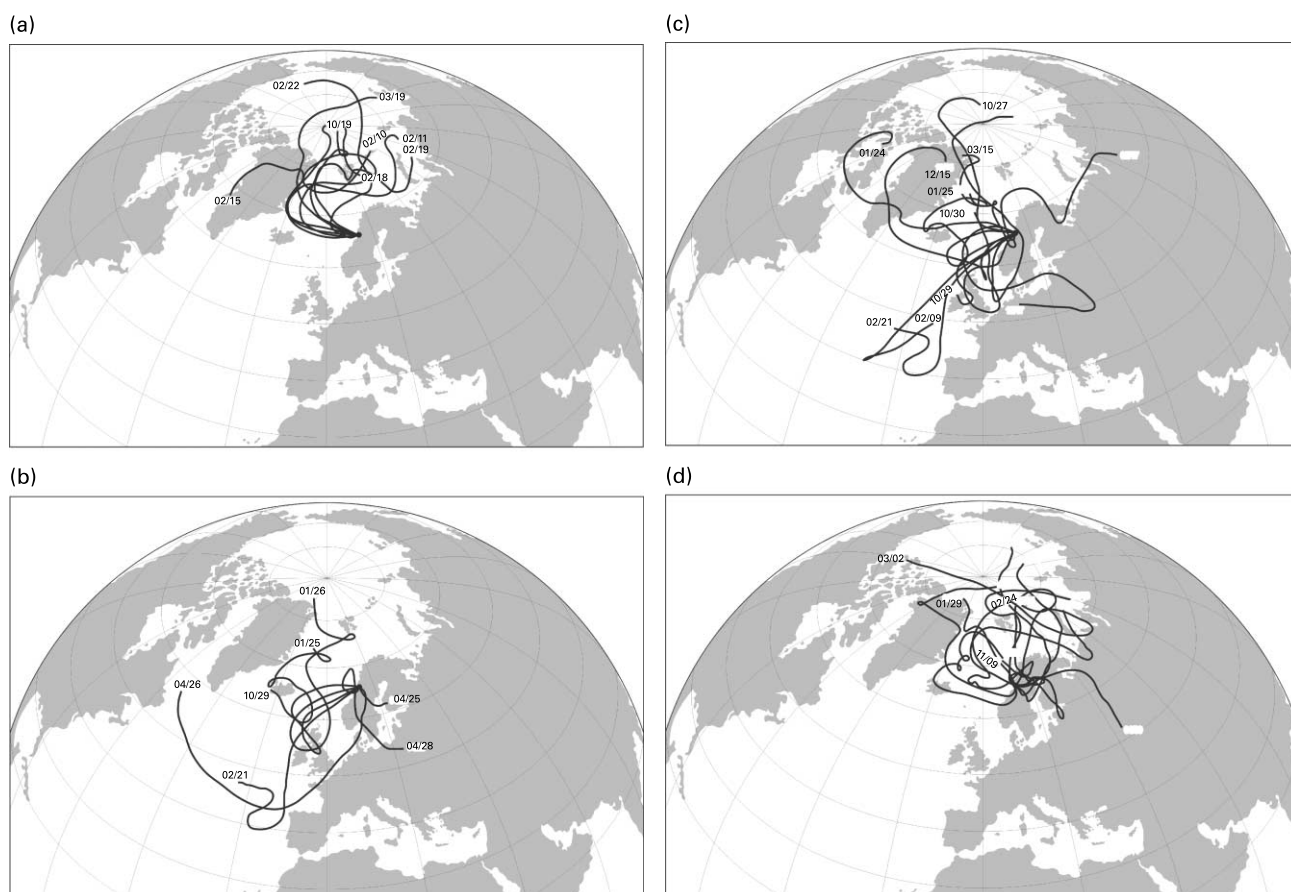


Figure 6 | 7-day trajectories of air masses arriving at a height of 500 m at Tustervatn at 18:00 hours on the indicated date. (a) Days with the highest Na^+ loads in precipitation at Tustervatn; (b) days with the highest nssSO_4^{2-} loads in precipitation at Tustervatn; (c) days on which the $\delta^{18}\text{O}$ values of precipitation at Tustervatn were $\geq 8\%$; (d) days on which the $\delta^{18}\text{O}$ values of precipitation at Tustervatn were $\leq -18\%$.

precipitation amount, suggest that this inability to make accurate load or flux calculations for ice cores does not have a significant effect on paleoclimate interpretations.

Dating the Austre Okstindbreen snowpack

The small size of the areas above and upwind of the 1470 m site on Austre Okstindbreen limits the possibility of snow drifting into it. Winds must have transported some snow away from the site, but the amount is not expected to have been a significant proportion of the total accumulation; most of the 4.8 m of sampled snow is likely to have accumulated *in situ*. The probability of surface melting at 1470 m between 8 October 1997 and 6 May 1998 is very low (Figure 5) and elution of ions is unlikely to have caused significant modification of the original stratigraphic chemistry. A

comparison of the stratigraphic variations of snow composition at Austre Okstindbreen and the temporal record of precipitation chemistry at Tustervatn, where only 24 mm (2.9%) of the winter's precipitation was not analysed for ions and 65 mm (8.0%) was not subject to oxygen isotope analysis, therefore was expected to yield information about the accumulation history of the snowpack on the glacier.

Dates and probable moisture transport routes can be assigned to parts of the Austre Okstindbreen snowpack on the basis of similarities between the chemical stratigraphy at 1470 m and the temporal variations of precipitation chemistry at Tustervatn (Figures 2–4). The first identifiable event is associated with an air mass that brought precipitation to Tustervatn on 19 October, having had a 7-day trajectory starting close to the North Pole, crossing the Denmark Strait and then tracking eastwards over the Norwegian Sea (Figure

6(a)). The resultant Na^+ load at Tustervatn is mirrored at around 3% WEOD in the Austre Okstindbreen snowpack (Figure 2). The last identifiable events are associated with air masses that crossed the Scandinavian land mass (Figure 6(b)) and brought high nssSO_4^{2-} loads to Tustervatn on 25, 26 and 28 April (Figure 3); the high nssSO_4^{2-} loads at 95–96% WEOD in the Austre Okstindbreen snowpack (Figure 3) can be assigned to this late-April period.

The high nssSO_4^{2-} loads associated with the very heavy precipitation at Tustervatn on 25 and 26 January are evident at around 40% WEOD (Figure 3). The air masses responsible for the event had moved southwards from the Arctic basin before crossing the United Kingdom on their way to Tustervatn (Figure 6(b)). The precipitation of 10 February, from an air mass which had a circuitous route around Svalbard before tracking westwards to the Greenland coast and then crossing the Norwegian Sea (Figure 6(a)), brought the winter's highest Na^+ load to Tustervatn; it can be traced at 51–52% WEOD in the Austre Okstindbreen snowpack (Figure 2). Peaks between 50% and 70% WEOD in the Na^+ stratigraphic profile at the 1470 m site correspond to the high Na^+ loads in precipitation at Tustervatn between 15 and 22 February (Figure 2).

The isotopic variations in the snowpack provide a substantial number of links to the precipitation record at Tustervatn (Figure 4). The minimum $\delta^{18}\text{O}$ value at 79% WEOD corresponds to the precipitation of 4 March at Tustervatn and the maximum at 84% WEOD to that of 15 March. Both events were associated with air masses that had 7-day trajectories from the Arctic basin to Tustervatn (Figure 6). 14.01 mm of precipitation fell at Tustervatn on 24 January, 18.79 mm on 25 January and 38.05 mm on 26 January, with $\delta^{18}\text{O}$ values of -6.66‰ , -5.77‰ and -12.21‰ , respectively. As many as twelve snowpack samples between about 35% and 45% WEOD probably date from this period; they are characterised by a series of increasing and then decreasing $\delta^{18}\text{O}$ values (Figure 4). On 25 and 26 February, precipitation at Tustervatn amounted to 54.49 mm and 8.89 mm, respectively, with $\delta^{18}\text{O}$ values of -8.04‰ and -8.06‰ ; again, several snowpack samples (at 71–79% WEOD) equate to the event (Figure 4). The increase of the $\delta^{18}\text{O}$ values during both this event and that of 25–26 January is characteristic of precipitation from a warm front during winter storms (Gedzelman & Lawrence 1982).

Differences of chemical inputs to the Tustervatn and Austre Okstindbreen sites

The influence that many daily precipitation events had at both Tustervatn and the 1470 m snowpack is evident in the ionic and isotopic records. However, it is clear that there were some differences of chemical inputs to the two sites. Substances emitted at ground level cannot reach high-elevation sites in winter because the lower troposphere is rather stable and up-slope winds are practically absent (Nickus *et al.* 1997). Furthermore, the trajectories of air masses arriving at 1470 m may differ from those arriving at 439 m. Accordingly, seven-day trajectories of air masses arriving at Tustervatn at 1500 m asl were examined to determine if they differed substantially from those arriving at 500 m asl. For most days, differences of the trajectories were relatively slight, but occasional striking departures were noted. The absence of a 'peak' nssSO_4^{2-} load and a high $\delta^{18}\text{O}$ value in the 1470 m snowpack to match those recorded at Tustervatn on 12 January (Figures 3 and 4) may be accounted for by the differing trajectories: that at 500 m had crossed Spain and the United Kingdom, whilst that arriving at 1500 m had passed over the Atlantic Ocean west of Ireland and had not crossed land surfaces. The 500 m trajectory arriving on 13 February passed over the Arctic Sea from the Barents Sea, whilst the 1500 m trajectory crossed Sweden; the small amount of precipitation at Tustervatn was heavily depleted of ^{18}O , and the absence of a corresponding pattern in the 1470 m record (Figure 4) probably reflects the difference of the trajectories. The 500 m trajectory arriving on 21 February 'started' to the west of Spain and passed close to the UK, whilst the 1500 m trajectory passed from Svalbard to Iceland en route to Tustervatn; the difference accounts for the absence in the 1470 m snowpack of the high nssSO_4^{2-} load, accompanied by a high $\delta^{18}\text{O}$ value, recorded at Tustervatn (Figures 3 and 4).

CONCLUSIONS

Moisture arriving in the Okstindan area has multiple sources and a variety of transport routes. Analysis of the trajectories of the air masses responsible for precipitation during discrete winter events revealed the coupling between atmospheric circulation and winter precipitation. Trajectories responsible for high Na^+ loads in precipitation at Tustervatn arrived from the west; those with high nssSO_4^{2-} loads had crossed the land

masses of Scandinavia and/or the United Kingdom. The highest nssSO_4^{2-} loads arrived at the end of the winter season in the Okstindan area, when much of southern Scandinavia already was free of snow and opportunities for acquisition of contaminants had increased. The lowest $\delta^{18}\text{O}$ values were associated with trajectories crossing the Greenland or Barents Seas en route from the Arctic basin; high $\delta^{18}\text{O}$ values resulted when trajectories arrived from the south-west or west.

Daily ionic loads were much more strongly related to the ionic composition of precipitation than to precipitation amount: whilst the Na^+ concentration at 1470 m asl was less than half that at Tustervatn, the total Na^+ load was >10% higher, as precipitation was almost 3 times that at the lower site.

Comparison of the temporal variations of oxygen isotopes and ions in daily precipitation at Tustervatn (439 m asl) and the stratigraphic variations of isotopes and ions in the snowpack at 1470 m asl on the Austre Okstindbreen glacier permitted the establishment of a detailed chronology of the snowpack stratigraphy. Sampling the accumulated snow at 5 cm intervals resulted in the analysis of several samples from a single day's precipitation. The ability to examine the influence of individual storms on $\delta^{18}\text{O}$ variations provided by the event-based (daily) data at Tustervatn and the detailed stratigraphical analysis of snowpack chemistry on Austre Okstindbreen illustrates the potential importance of such high-resolution temporal data in relation to understanding past, present and possible future climatic conditions.

ACKNOWLEDGEMENTS

I am grateful to Peter Raben and Lars Thomsen for meticulous work in difficult conditions at Austre Okstindbreen, and to Ari Tustervatn for his diligence in collecting samples for isotope analysis. Considerable help was provided by Kjetil Tørseth and Jan Erik Hanssen at NILU, by Tvis Knudsen at the Earth Science Institute, Aarhus University, and by staff at the Niels Bohr Institute, University of Copenhagen. Trajectory data were provided by EMEP, a co-operative project for monitoring and evaluating long-range transport of air pollutants in Norway, using the FLEXTRA model developed by A. Stohl. I thank Nick Scarle for drafting the figures. Constructive comments by two anonymous reviewers improved the paper.

REFERENCES

- Aizen, V. B., Aizen, E., Fujita, K., Stanislav, A., Nikitin, A., Kreutz, K. J. & Takeuchi, L. N. 2005 Stable-isotope time series and precipitation origin from firn-core and snow samples, Altai glaciers, Siberia. *J. Glaciol.* **51**, 637–654.
- Araguas-Araguas, L., Froehlich, K. & Rozanski, K. 2000 Deuterium and oxygen-18 isotope composition of precipitation and atmospheric moisture. *Hydrol. Proc.* **14**, 1341–1355.
- Asaf, L., Nativ, B., Hassan, M. A., Shain, D., Geyer, S. & Ziv, B. 2005 Influence of small- and large-scale variables on the chemical and isotopic composition of urban rainwater, as illustrated by a case study in Ashod, Israel. *J. Geophys. Res.* **110**, D110, doi:10.1029/2004JD005414.
- Burnett, A. W., Mullins, H. J. & Patterson, W. P. 2004 Relationship between atmospheric circulation and winter precipitation $\delta^{18}\text{O}$ in central New York State. *Geophys. Res. Lett.* **31**, L22209, doi: 10.1029/2004GL021089.
- Cole, J. E., Rind, D., Webb, R. S., Jouzel, J. & Healy, R. 1999 Climatic controls on interannual variability of precipitation $\delta^{18}\text{O}$: simulated influence of temperature, precipitation amount, and vapour source region. *J. Geophys. Res.* **104**(D12), 14 223–14 235.
- Cuffey, K. M., Clow, G. D., Alley, R. B., Stuiver, M., Waddington, E. D. & Saltus, R. W. 1995 Large arctic temperature change at the Wisconsin-Holocene glacial transition. *Science* **270**, 455–458.
- Dansgaard, W. 1964 Stable isotopes in precipitation. *Tellus* **16**, 436–438.
- Dorling, S. R., Davies, T. D. & Pierce, C. E. 1992 Cluster analysis: a technique for estimating the synoptic meteorological controls on air and precipitation chemistry - method and application. *Atmos. Environ.* **26A**, 2575–2581.
- Fricke, H. C. & O'Neil, J. R. 1999 The correlation between $^{18}\text{O}/^{16}\text{O}$ ratios of meteoric water and surface temperature: its use in investigating terrestrial climate change over geologic time. *Earth Planet. Sci. Lett.* **170**, 181–196.
- Gat, J. R. 1996 Oxygen and hydrogen isotopes in the hydrologic cycle. *Ann. Rev. Earth Planet. Sci.* **24**, 225–262.
- Gedzelman, S. D. & Lawrence, J. R. 1982 The isotopic composition of cyclonic precipitation. *J. Appl. Meteorol.* **21**, 1385–1404.
- Hammer, C. U., Clausen, H. B., Dansgaard, W., Gundestrup, N., Johnsen, S. J. & Reeh, N. 1978 Dating of Greenland ice cores by flow models, isotopes, volcanic debris and continental dust. *J. Glaciol.* **20**, 3–26.
- He, Y. & Theakstone, W. H. 1994 Climatic influence on the composition of snow cover at Austre Okstindbreen, Norway, 1989 and 1990. *Ann. Glaciol.* **19**, 1–6.
- Hoffmann, G., Jouzel, J. & Masson, V. 2000 Stable water isotopes in general circulation models. *Hydrol. Process.* **14**, 1385–1406.
- Kahl, J. D. W., Martinez, D. A., Kuhns, H., Davidson, C. I., Jaffrezo, J.-L. & Harris, J. M. 1997 Air mass trajectories to Summit Greenland: a 44-year climatology and some episodic events. *J. Geophys. Res.* **102**(C12), 26 861–26 873.
- Knudsen, N. T. 2000 Okstindan. In: Andreassen, L. M. (ed.) *Regional Changes of Glaciers in Northern Norway*. Norwegian Water

- Resources and Energy Directorate Report 2000 No. 1. Norwegian Water Resources and Energy Directorate, Oslo, pp. 15–27.
- Krupa, S. V. 2002 Sampling and physico-chemical analysis of precipitation: a review. *Environ. Pollut.* **120**, 565–594.
- Maupetit, F. & Delmas, R. J. 1994 Snow chemistry of high altitude glaciers in the French Alps. *Tellus* **46B**, 304–324.
- Nickus, U., *et al.* 1997 SNOsP: Ion deposition and concentration in high alpine snow packs. *Tellus* **49B**, 56–71.
- Norman, M., Das, S. N., Pillai, A. G., Granat, L. & Rohde, H. 2001 Influence of air mass trajectories on the chemical composition of precipitation in India. *Atmos. Environ.* **35**, 4223–4235.
- Preunkert, S., Wagenbach, D., Legrand, M. & Vincent, C. 2000 Col du Dôme (Mt Blanc Massif French Alps) suitability for ice-core studies in relation with past atmospheric chemistry over Europe. *Tellus* **52B**, 993–1012.
- Raben, P. & Theakstone, W. H. 1994 Isotopic and ionic changes in a snow cover at different altitudes: observations at Austre Okstindbreen in 1991. *Ann. Glaciol.* **19**, 85–91.
- Raben, P. & Theakstone, W. H. 1998 Changes of ionic and oxygen isotopic composition of the snowpack at the glacier Austre Okstindbreen, Norway, 1995. *Nordic Hydrol.* **29**, 1–20.
- Raben, P., Tørseth, K. & Theakstone, W. H. 2000 Relations between winter climate and ionic variations in a seven-meter-deep snowpack at Okstindan, Norway 1995. *Arc. Antarc. Alp. Res.* **32**, 189–196.
- Rozanski, K., Araguas-Araguas, L. & Gonfiantini, R. 1993 Isotope patterns in modern global precipitation. *Geophys. Monograph* **78**, 1–36.
- Rozanski, K., Sonntag, G. & Münich, K. O. 1982 Factors controlling stable isotope composition of European precipitation. *Tellus* **34**, 142–150.
- Stohl, A., Wotawa, G., Seibert, P. & Kromp-Kolb, H. 1995 Interpolation errors in wind fields as a function of spatial and temporal resolution and their impact on different types of kinematic trajectories. *J. Appl. Meteorol.* **34**, 2149–2165.
- Theakstone, W. H. 1988 Temporal variations of isotopic composition of glacier-river water during summer: observations at Austre Okstindbreen Okstindan, Norway. *J. Glaciol.* **34**, 309–317.
- Theakstone, W. H. 2003 Oxygen isotopes in glacier-river water, Austre Okstindbreen, Okstindan, Norway. *J. Glaciol.* **49**, 282–298.
- Theakstone, W. H. & Knudsen, N. T. 1996a Oxygen isotope and ionic concentrations in glacier river water: multi-year observations in the Austre Okstindbreen basin Okstindan, Norway. *Nordic Hydrol.* **27**, 101–116.
- Theakstone, W. H. & Knudsen, N. T. 1996b Isotopic and ionic variations in glacier river water during three contrasting ablation seasons. *Hydrol. Process.* **10**, 523–539.
- Tørseth, K. 1996 *Overvåking av langtransportert forurensning i luft og nedbør. Atmosfærisk tilførsel, 1995.* Statlig program for forurensnings overvåking. Rapport. Kjeller, NILU OR38/96.
- Tørseth, K., Hanssen, J. E. & Semb, A. 1999 Temporal and spatial variations of airborne Mg, Cl, Na, Ca and K in rural areas in Norway. *Sci. Total Environ.* **234**, 75–85.
- Tørseth, K. & Semb, A. 1995 Sulphur and nitrogen deposition in Norway: status and trends. *Wat. Air Soil Pollut.* **85**, 623–628.
- Yoshimura, K., Oki, T. & Ichiyonagi, K. 2004 Evaluation of two-dimensional atmospheric water circulation fields in reanalyses by using precipitation isotope databases. *J. Geophys. Res.* **109**(D20), art. D20209.

First received 30 May 2007; accepted in revised form 20 November 2007